

Upstream neutrino production and delayed jet emission in the blazar GB6 J1542+6129

Downloaded from: https://research.chalmers.se, 2026-11-09 00:29 UTC

Citation for the original published paper (version of record):
Kun, E., Bartos, I., Hadi, B. et al (2026). Upstream neutrino production and delayed jet emission in the blazar GB6 J1542+6129. Astronomy and Astrophysics, 714.
http://dx.doi.org/10.1051/0004-6361/202660739

N.B. When citing this work, cite the original published paper.

research.chalmers.se offers the possibility of retrieving research publications produced at Chalmers University of Technology. It covers all kind of research output: articles, dissertations, conference papers, reports etc. since 2004. research.chalmers.se is administrated and maintained by Chalmers Library

(article starts on next page)

A&A, 714, A174 (2026)
https://doi.org/10.1051/0004-6361/202660739
© The Authors 2026

Astronomy & Astrophysics

Upstream neutrino production and delayed jet emission in the blazar GB6 J1542+6129

Emma Kun[1,2,3,4,⋆], Imre Bartos[5], Breshna Hadi[6], Anna Göblyös[7], Julia Becker Tjus[4,8,9], Peter L. Biermann[10,11], Anna Franckowiak[6], Francis Halzen[12], Santiago del Palacio[9], and Claudio Ricci[13,14]

[1] Department of Astronomy, Institute of Physics and Astronomy, ELTE, Pázmány Péter sétány 1a, 1117 Budapest, Hungary
[2] Konkoly Observatory, HUN-REN Research Centre for Astronomy and Earth Sciences, Konkoly Thege Miklós út 15–17, 1121 Budapest, Hungary
[3] CSFK, MTA Centre of Excellence, Konkoly Thege Miklós út 15–17, 1121 Budapest, Hungary
[4] Theoretical Physics IV, Faculty for Physics & Astronomy, Ruhr University Bochum, 44801 Bochum, Germany
[5] Department of Physics, University of Florida, PO Box 118440, Gainesville, FL 32611-8440, USA
[6] Astronomical Institute, Faculty for Physics & Astronomy, Ruhr University Bochum, 44780 Bochum, Germany
[7] Institute of Physics, University of Szeged, Szeged, Hungary
[8] Ruhr Astroparticle And Plasma Physics Center (RAPP Center), Ruhr University Bochum, 44801 Bochum, Germany
[9] Department of Space, Earth and Environment, Chalmers University of Technology, 412 96 Gothenburg, Sweden
[10] Max Planck Institute for Radio Astronomy, 53121 Bonn, Germany
[11] Department of Physics & Astronomy, University of Alabama, Tuscaloosa, AL 35487, USA
[12] Department of Physics, University of Wisconsin, Madison, WI 53706, USA
[13] Department of Astronomy, University of Geneva, 1205 Geneva, Switzerland
[14] Instituto de Estudios Astrofísicos, Facultad de Ingeniería y Ciencias, Universidad Diego Portales, Av. Ejército Libertador 441, Santiago, Chile

Received 1 May 2026 / Accepted 5 August 2026

ABSTRACT

Aims. We present a multimessenger case study of the blazar GB6 J1542+6129. We examined whether its multiwavelength behavior is consistent with neutrino production in a compact region near the central black hole or with the parsec-scale radio jet.
Methods. We performed a multimessenger analysis combining ∼17 years of *Fermi*-LAT γ-ray data, including a 5% adaptively binned light curve and Bayesian block decomposition, with ∼14 years of VLBI/MOJAVE observations to derive the Doppler factor evolution of the radio core. These were compared to the temporal properties of a suspected IceCube neutrino flare with a duration of 147^{+110}_{-25} days, enabling a direct test of spatial and causal connections between neutrino and electromagnetic emission regions.
Results. The suspected neutrino flare appears to precede a γ-ray flare and a pronounced increase in the very long baseline (VLBI) core Doppler factor by up to ∼1 year. The duration of the post-flare γ-ray activity is comparable to that of the neutrino flare, which in our framework is consistent with both signatures originating from a single propagating disturbance whose temporal structure is preserved during the propagation, rather than being set by the light-crossing time of any single emission zone. The γ-ray spectral energy distribution remains consistent in shape in the full, flare, and post-flare intervals, indicating stable particle acceleration conditions. The temporal ordering, taken at face value, places the neutrino production site upstream of the VLBI core.
Conclusions. The observations of GB6 J1542+6129 are consistent with a disturbance-driven multi-zone scenario in which neutrinos are produced in a compact photon-rich inner region upstream of the parsec-scale VLBI core, plausibly in the coronal region, while the same disturbance later enhances Doppler-boosted leptonic emission when it reaches the radio core. While the data alone do not strictly establish this scenario on a population level, they show how time-domain multi-messenger observations of a single active galactic nucleus can localize neutrino emission relative to the parsec-scale radio jet in a particular source.

Key words. neutrinos – radiation mechanisms: non-thermal – galaxies: active – galaxies: jets – gamma rays: galaxies – radio continuum: galaxies

1. Introduction

Since the discovery of the diffuse astrophysical neutrino flux by IceCube (IceCube Collaboration 2013), it has become a central challenge of multi-messenger astrophysics to identify its sources. Active galactic nuclei (AGNs), powered by accreting supermassive black holes, are among the promising candidates for the production of cosmic neutrinos (e.g. Begelman et al. 1984). Their compact central regions host dense radiation fields, while relativistic jets in radio-loud AGNs provide additional sites for particle acceleration. However, the dominant physical conditions and locations of neutrino production within AGNs remain unresolved. Discovery-level associations, such as with the blazar TXS 0506+056 and the Seyfert galaxy NGC 1068, demonstrated that radio-loud and radio-quiet AGNs can produce detectable high-energy neutrinos (IceCube Collaboration 2018; Abbasi et al. 2022).

Effective high-energy neutrino production is expected to occur in compact regions close to the central black hole, where dense radiation fields, for instance, from the accretion disk, broad-line region, and X-ray corona, provide abundant target photons for proton–photon ($p\gamma$) interactions. Relativistic

⋆ Corresponding author: kun.emma@csfk.org

Open Access article, published by EDP Sciences, under the terms of the Creative Commons Attribution License (https://creativecommons.org/licenses/by/4.0), which permits unrestricted use, distribution, and reproduction in any medium, provided the original work is properly cited.
This article is published in open access under the Subscribe to Open model. Subscribe to A&A to support open access publication.

protons, accelerated to PeV–EeV energies by shocks, magnetic reconnection, or shear flows in the jet base, interact with these ambient photons predominantly via the Δ^+ resonance, $p + \gamma \rightarrow \Delta^+ \rightarrow n\pi^+$ or $p\pi^0$. Charged pions decay as $\pi^+ \rightarrow \mu^+ + \nu_\mu$ followed by $\mu^+ \rightarrow e^+ + \nu_e + \bar{\nu}_\mu$, yielding high-energy neutrinos that each carry ∼5% of the parent proton energy, while neutral pions decay into photon pairs ($\pi^0 \rightarrow 2\gamma$) that initiate the accompanying electromagnetic cascade. In such environments, high-energy γ rays are efficiently absorbed (Kun et al. 2021, 2023) and reprocessed to lower energies, while neutrinos escape unattenuated (e.g. Stecker et al. 1991; Murase & Waxman 2016; Murase 2022). This naturally links neutrino emission to intrinsic hard X-ray radiation tracing compact photon fields. Observational evidence of a hard X-ray–high-energy neutrino correlation was first established in three Seyfert galaxies (NGC 1068, NGC 3079, and NGC 4151) by Neronov et al. (2024) and was later extended to a broader population including Seyferts (e.g., CGCG 420-015) and blazars such as TXS 0506+056 and GB6 J1542+6129 (Kun et al. 2024).

In this work, we present a multi-messenger analysis of GB6 J1542+6129 for which we combined *Fermi*-LAT γ-ray variability, very long baseline interferometry (VLBI) Doppler factor evolution, and IceCube constraints. The blazar GB6 J1542+6129 (z=0.507) is a candidate neutrino emitter. Time-integrated searches in 10 years of IceCube data report significances for GB6 J1542+6129 of $p \approx 0.0018$ (pre-trial) when using the 2008–2018 dataset, which includes partial-detector data from 2008–2011 (Aartsen et al. 2020), and $p \approx 0.0126$ when restricted to the full-detector data collected between 2011 and 2020 (Abbasi et al. 2022). The IceCube multi-flare analysis identifies a flare peaking on 2016-12-18 with duration 147^{+110}_{-25} days at a pre-trial significance of $p \approx 0.0021$ (Abbasi et al. 2021). In these searches, GB6 J1542+6129 is the fourth strongest neutrino association in the IceCube source list. Together with its position on the proposed hard X-ray–neutrino luminosity relation (Kun et al. 2024), this makes GB6 J1542+6129 a prime target for studying whether the multi-messenger behavior of a candidate neutrino blazar is consistent with neutrino production in a compact photon-rich inner region.

2. Fermi-LAT gamma-ray light curve

We analyzed ∼17 yr of *Fermi*-LAT data of GB6 J1542+6129, covering the time interval from 2008 August to 2025 June (Abdollahi et al. 2020). Events were selected in the energy range 100 MeV–800 GeV within a 20° region of interest centered on the source position. Standard quality cuts were applied, including `evclass=128` (P8R3 SOURCE class), `evtype=3` (FRONT+BACK events), and a zenith angle cut at 90° to suppress contamination from the Earth limb. The analysis was performed using a binned likelihood approach within the `fermiPy` framework, incorporating the standard Galactic and isotropic diffuse background models as well as cataloged point sources in the region. The minimum detection threshold for inclusion of new point sources in the model of the region of interest was TS=16. Initial light curves were produced using a fixed time binning (28, 56, and 84 days), revealing significant variability but also a fraction of low-significance (TS < 16) data points.

To obtain a statistically robust representation of the source variability, we constructed an adaptively binned light curve following a constant relative flux uncertainty criterion of 5%. In this method, the widths of the time bins are adjusted so that each bin satisfies $\Delta F/F \approx 0.05$ in an initial approximate likelihood fit, ensuring approximately uniform statistical significance throughout the light curve. This approach maximizes the temporal resolution during high-flux states while preserving sensitivity during low-flux periods. The uncertainties in the flux measurements are obtained directly from the likelihood profile and correspond to statistical (1σ) errors. The fluxes in each bin were derived from likelihood fits assuming a power-law spectral model, and only bins with a reliable convergence were retained. We show the resulting *Fermi*-LAT γ-ray light curve of GB6 J1542+6129 in Fig. 1. The resulting adaptively binned light curve reveals pronounced gamma-ray flaring activity, with enhanced emission episodes following the neutrino flare epoch.

3. Analysis of the archival VLBI data

We analyzed archival 15.368 GHz Very Long Baseline Array (VLBA) data from the Monitoring Of Jets in Active galactic nuclei with VLBA Experiments (MOJAVE) survey (Lister et al. 2018), covering ∼14 yr of observations of GB6 J1542+6129. The calibrated visibility data were self-calibrated and imaged with `DIFMAP` (Shepherd 1997), and the brightness distribution was modeled with circular Gaussian components fitted to the visibilities. The innermost component was identified as the VLBI core.

For each epoch, we derived the flux density S_ν, sky position, and angular size d of the jet component. The Doppler factor of the VLBI core δ was estimated from its brightness temperature,

$$T_{\rm b,VLBI} = 1.22 \times 10^{12} (1+z) \frac{S_\nu}{d^2 \nu^2} \ {\rm K}. \quad (1)$$

Following Readhead (1994), we adopted the equipartition value $T_{\rm eq} = 5 \times 10^{10}$ K, which corresponds to the state in which the energy densities of the radiating relativistic electrons and the magnetic field are comparable. This choice was motivated by theoretical and observational arguments: synchrotron sources tend to evolve toward equipartition because departures from it are energetically unfavorable and short-lived (Readhead 1994), and statistical studies of large VLBI samples reported intrinsic brightness temperatures clustered close to this value when Doppler boosting was accounted for (e.g. Homan et al. 2006; Liodakis et al. 2018). We caution, however, that this assumption is best motivated for the typical (long-term quiescent) brightness and not for the flaring state. During active phases, blazar cores can depart from equipartition toward higher intrinsic brightness temperatures, up to the inverse-Compton limit $T_{\rm IC} \sim 5 \times 10^{11}$ K (Kellermann & Pauliny-Toth 1969).

We show the evolution of the Doppler factor of the VLBI core of GB6 J1542+6129 in Fig. 1. The evolution of the Doppler factor is characterized by moderate values ($\delta \sim 1$–10) in most epochs, but exhibits a pronounced peak at epoch 2018.092, reaching $\delta_{\rm core} = 42.6 \pm 8.6$ under the equipartition assumption, with the core size above the minimum resolvable size. As explained above, the peak value should therefore be regarded as an upper limit on the Doppler factor. The uncertainties on δ were derived via error propagation, accounting for measurement errors on S_ν and d, as well as the uncertainty introduced by the resolution limit. We note that only a single MOJAVE epoch falls within the flaring interval, which limits the temporal resolution at which the Doppler-factor evolution can be reconstructed for the whole flare.

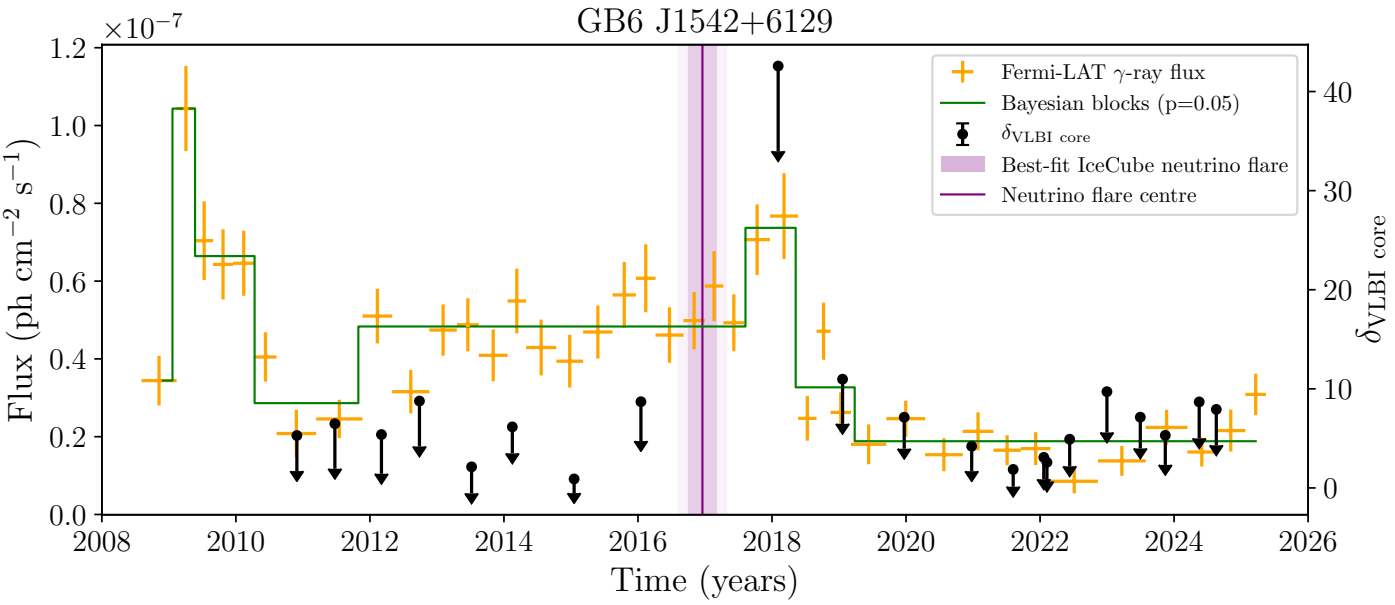


Fig. 1. Multi-messenger temporal evolution of the blazar GB6 J1542+6129. The orange points (left axis) show the adaptively binned *Fermi*-LAT γ-ray flux (100 MeV–800 GeV), constructed with a constant 5% relative uncertainty criterion. The green lines show the Bayesian blocks with $p = 0.05$. The black points (right axis) show the Doppler factor of the VLBI core derived from 15 GHz MOJAVE observations. Under the equipartition assumption (Sect. 3), these are upper limits, indicated by downward arrows, and should not be read as direct measurements; the data are formally consistent with a constant Doppler factor. We also note the absence of VLBI epochs between early 2016 and 2018, which prevents a precise localization of the epoch of peak core brightness. The vertical purple line marks the central epoch of the suspected IceCube neutrino flare (Abbasi et al. 2021), and the shaded regions indicate its central duration of 147 d (darker band) and its 1σ upper extent of 257 d (lighter band). The observed temporal offset indicates that the neutrino emission occurs earlier than the subsequent electromagnetic activity.

4. Discussion

We combined *Fermi*-LAT γ-ray observations with VLBI measurements of the jet structure to investigate the origin of the high-energy emission in GB6 J1542+6129. The 5% adaptively binned γ-ray light curve and the time evolution of the VLBI core Doppler factor are shown in Fig. 1. The VLBI core marks the surface where the jet becomes optically thin at the observing frequency and is typically treated as stationary.

Changes in the brightness temperature could in principle arise from variations in jet orientation, but the VLBI data disfavor this: the jet direction remains stable, with no clear outward motion or structural evolution, and the core flux density rises concurrently with the apparent Doppler factor. Since the total radio emission is strongly core-dominated and the jet ridge line is unchanged, we interpret the enhancement as a transient brightening of the VLBI core associated with the passage of a disturbance, reflecting some combination of enhanced Doppler boosting, increased emissivity, and a possible intrinsic departure from equipartition during the active state and not a geometric viewing-angle swing.

The multi-messenger data are temporally ordered: the suspected neutrino flare appears to precede the γ-ray enhancement and the VLBI Doppler-factor peak by up to ∼1 year. We emphasize that the available data, in particular, the limited cadence of the MOJAVE observations of the flare, prevented us from measuring the γ-ray–radio delay (or the neutrino–radio delay) with precision; our argument rests on the ordering of the neutrino flare center relative to the peak of the electromagnetic activity, not on a precise delay measurement. In particular, no VLBI epochs are available between early 2016 and 2018 (Fig. 1), so the epoch of peak core brightness is only loosely localized: the implied neutrino-to-radio ordering could range from the ∼1 yr quoted here to zero, or even to slightly negative values on the order of half a year. We therefore treat the ∼1 yr figure as an indicative upper estimate of the ordering rather than a measured delay. This sampling limitation specifically applies to the neutrino-to-radio ordering. The γ-ray flare itself is well localized to ∼2018 by the *Fermi* LAT light curve; the radio peak, by contrast, is poorly localized because of the VLBI gap and could in principle precede the γ-ray flare. We therefore do not claim an observed radio–γ-ray simultaneity. Rather, in the synchrotron self-Compton picture developed below, the radio and γ-ray enhancements are co-spatial and hence expected to be nearly simultaneous. This is a prediction of the scenario that the sparse VLBI sampling can neither confirm nor refute.

With this caveat, the ∼1 year ordering is naturally interpreted as the propagation time of a disturbance, for example, a traveling shock, magnetic reconnection event, or plasmoid, moving outward along the jet. By “disturbance” we mean a localized transient enhancement in the density and/or energy of the relativistic particle population, physically realized as a traveling shock, magnetic reconnection event, or plasmoid. At the neutrino production site in the compact inner region, the disturbance need not yet be ultra-relativistic: it accelerates protons close to the black hole, where the dense radiation fields make $p\gamma$ interactions efficient, and it only subsequently becomes entrained in the fast bulk-jet flow as it propagates to parsec scales. The mildly relativistic effective velocities inferred above are consistent with this picture. Close to the black hole, the dense radiation fields of the accretion disk, broad-line region, and corona provide abundant target photons for $p\gamma$ interactions, so a disturbance that accelerates protons there immediately produces neutrinos, while co-spatial GeV γ-rays are absorbed via $\gamma\gamma \rightarrow e^+e^-$ pair production in the same photon fields. As the disturbance propagates

outward and the emission region becomes transparent to GeV photons, the γ-ray flare emerges with a delay set by the light-travel time between the opaque inner zone and the transparent outer jet.

In this picture, the γ-ray emission seen during the flare is the disturbance-enhanced component, produced where the propagating disturbance reaches the parsec-scale radio core (e.g. Marscher et al. 2008; Agudo et al. 2011), rather than the steady-state inner-jet emission expected at hundreds of Schwarzschild radii in canonical high-power blazar models (e.g. Ghisellini & Tavecchio 2009). The radio core marks the frequency-dependent $\tau \approx 1$ surface at which the jet becomes optically thin to synchrotron self-absorption at 15 GHz (Blandford & Königl 1979; Lobanov 1998). At this location, the transiently enhanced population of relativistic electrons produces the radio flare, and part of the same synchrotron photon field is up-scattered to GeV γ-ray energies via the synchrotron self-Compton process. The radio and γ-ray enhancements are therefore expected to be essentially co-spatial, both originating at the radio core: when the region is optically thin to the 15 GHz radio photons, it is also transparent to the resulting GeV γ-rays. The spatial separation in our scenario is thus between the upstream neutrino production site (the compact γ-obscured inner region) and the downstream radio or γ-ray zone at the parsec-scale core and not between the radio and γ-ray emission themselves. Internal shocks (Sikora et al. 1994; Spada et al. 2001) and magnetic reconnection in magnetically dominated jets (e.g. Sironi et al. 2016; Petropoulou et al. 2019) are both established mechanisms for producing such disturbances.

The disturbance path Δr, the observed delay $\Delta t_{\rm obs}$, and the disturbance velocity $\beta_{\rm shock}$ along the jet are related by

$$\Delta t_{\rm obs} = (1+z)\,\frac{\Delta r}{c}\left(\frac{1}{\beta_{\rm shock}} - \cos\theta\right). \tag{2}$$

The VLBI core at centimeter wavelengths typically sits at $\sim 10^3$–10^6 gravitational radii from the central black hole (Marscher et al. 2008; Hada et al. 2011), that is, $\Delta r \sim 0.025$–25 pc for an FSRQ-class blazar with $M_{\rm BH} \sim 5\times10^8\,M_\odot$ (e.g. Ghisellini et al. 2010; Zhang et al. 2024). Combined with $\Delta t_{\rm obs} \sim 1$ yr and a small viewing angle $\theta \sim 1/\Gamma_{\rm jet}$, this implies an effective disturbance velocity $\beta_{\rm shock} \sim 0.1$–$1$ within the geometric range. We stress that this range is essentially unconstrained by the present data: it only excludes a static or strongly sub-relativistic disturbance and is consistent with any mildly to highly relativistic propagation speed. A meaningful velocity constraint would require denser VLBI sampling of the whole flare. The mere existence of an observed delay is nonetheless informative: a strictly luminal disturbance viewed head-on would produce no time difference between the upstream neutrino emission and the downstream γ-ray flare because both would propagate at the speed of light from the same starting point.

The broadband spectral energy distributions (SEDs) during the full observational period, the neutrino-to-jet active interval (2016 January 16–2019 January 19), and the post-flare interval (2019–2025) are shown in Fig. 2. All three share a common log-parabola shape within the uncertainties on α and β, with only the normalization rising during the flare and dropping afterward. This is consistent with a stable emission region whose brightening reflects an increase in particle or energy density rather than spectral evolution. The comparable neutrino and γ-ray durations further suggest that the observed timescale traces the lifetime of the disturbance, not the light-crossing time of a stationary zone. After the flare, the VLBI core Doppler factor returns to its pre-flare baseline while the γ-ray flux settles at a systematically lower level, indicating that the long-term emission is governed by plasma conditions and not by boosting. This is consistent with a partial depletion of the downstream radiating population by the shock. The disturbance can also propagate through a preconditioned jet shaped by prior activity, producing intermittent highly nonuniform acceleration reminiscent of lightning-like processes in turbulent plasmas (Allen et al. 2024).

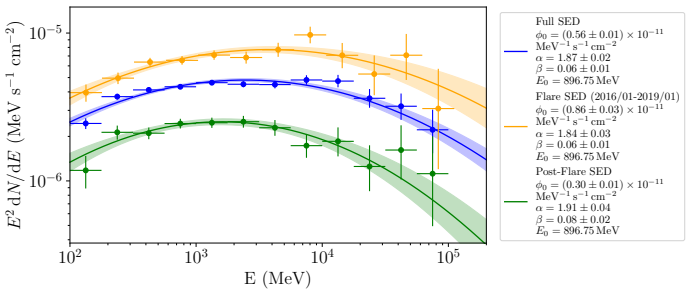


Fig. 2. Broadband SEDs of GB6 J1542+6129 during the full observational period (blue), during the neutrino-associated flare interval (orange), and during the post-flare interval (green). The data points represent the *Fermi*-LAT measurements in logarithmic energy bins, and the solid curves show the best-fit log-parabola models.

5. Conclusion

We presented a multi-messenger analysis of the high-energy neutrino source candidate blazar GB6 J1542+6129 for which we combined *Fermi*-LAT γ-ray observations, VLBI-based Doppler factor measurements, and IceCube neutrino data (see Fig. 1). Taken at face value, the data show a temporal ordering in which the suspected neutrino flare precedes the subsequent electromagnetic activity by $\sim$1 year. This delay, together with the comparable durations of the neutrino and γ-ray flares, is consistent with a single propagating disturbance whose temporal structure is preserved during transit from a compact inner emission region to the parsec-scale jet. In this picture, the delayed γ-ray emission, closely tracked by the Doppler-factor variability, is most naturally explained as Doppler-boosted leptonic radiation enhanced by the passage of the disturbance, while the neutrino emission traces hadronic processes in a compact γ-obscured inner region.

The observations are therefore consistent with a two-zone scenario in which a propagating disturbance produces neutrinos upstream and subsequently generates Doppler-boosted leptonic emission (plausibly including synchrotron self-Compton (SSC) and external Compton) as it propagates downstream. This framework naturally accommodates the observed time ordering, the correlation between γ-ray flux and Doppler factor (Fig. 1), and the SED stability in the activity states (Fig. 2). Combined with the geometric scale of the corona to the VLBI core ($\sim$0.025–25 pc for $M_{\rm BH} \sim 5\times10^8\,M_\odot$), the observed delay is consistent with a (sub)relativistic propagating disturbance, consistent with neutrino production in the coronal region, with the disturbance subsequently propagating outward through the inner jet to the parsec-scale VLBI core. The hard X-ray–neutrino luminosity relation of Kun et al. (2024), established on a broader AGN sample, provides empirical support for an origin in inner radiatively efficient regions. We emphasize that given the modest individual significance of the IceCube excess on this source and the limited cadence of the VLBI data during the flare,

our results constrain a scenario consistent with inner-zone neutrino production and disturbance-driven jet variability, but do not establish it. GB6 J1542+6129 nevertheless illustrates how time-domain multi-messenger observations can be used to localize the neutrino production site within an AGN.

Acknowledgements. We thank the anonymous referee for constructive feedback that improved this work. E.K. thanks funding from the NKFIH excellence grant TKP2021-NKTA-64. A. G. thanks support from the Pannónia Scholarship Programme. E.K., J.T. and A.F. acknowledge support from the German Science Foundation DFG, via the Collaborative Research Center *SFB1491: Cosmic Interacting Matters – from Source to Signal*. CR acknowledges support from SNSF Consolidator grant F01−13252 and ANID BASAL project FB210003. This paper makes use of publicly available Fermi-LAT data provided online by the Fermi Science Support Center. We acknowledge the use of the HUN-REN Cloud. This research has made use of data from the MOJAVE database that is maintained by the MOJAVE team (Lister et al. 2018). The National Radio Astronomy Observatory is a facility of the National Science Foundation operated under cooperative agreement by Associated Universities, Inc.

References

Aartsen, M. G., Ackermann, M., Adams, J., et al. 2020, Phys. Rev. Lett., 124, 051103
Abbasi, R., Ackermann, M., Adams, J., et al. 2021, ApJ, 920, L45
Abbasi, R., Ackermann, M., Adams, J., et al. 2022, Science, 378, 538
Abdollahi, S., Acero, F., Ackermann, M., et al. 2020, ApJS, 247, 33
Agudo, I., Jorstad, S. G., Marscher, A. P., et al. 2011, ApJ, 726, L13
Allen, M. L., Biermann, P. L., Chieffi, A., et al. 2024, Astropart. Phys., 161, 102976
Begelman, M. C., Blandford, R. D., & Rees, M. J. 1984, Rev. Mod. Phys., 56, 255
Blandford, R. D., & Königl, A. 1979, ApJ, 232, 34
Ghisellini, G., & Tavecchio, F. 2009, MNRAS, 397, 985
Ghisellini, G., Tavecchio, F., Foschini, L., et al. 2010, MNRAS, 402, 497
Hada, K., Doi, A., Kino, M., et al. 2011, Nature, 477, 185
Homan, D. C., Kovalev, Y. Y., Lister, M. L., et al. 2006, ApJ, 642, L115
IceCube Collaboration 2013, Science, 342, 1242856
IceCube Collaboration (Fermi-LAT, MAGIC, et al.) 2018, Science, 361, 147
Kellermann, K. I., & Pauliny-Toth, I. I. K. 1969, ApJ, 155, L71
Kun, E., Bartos, I., Tjus, J. B., et al. 2021, ApJ, 911, L18
Kun, E., Bartos, I., Becker Tjus, J., et al. 2023, A&A, 679, A46
Kun, E., Bartos, I., Tjus, J. B., et al. 2024, Phys. Rev. D, 110, 123014
Liodakis, I., Hovatta, T., Huppenkothen, D., et al. 2018, ApJ, 866, 137
Lister, M. L., Aller, M. F., Aller, H. D., et al. 2018, ApJS, 234, 12
Lobanov, A. P. 1998, A&A, 330, 79
Marscher, A. P., Jorstad, S. G., D'Arcangelo, F. D., et al. 2008, Nature, 452, 966
Murase, K. 2022, ApJ, 941, L17
Murase, K., & Waxman, E. 2016, Phys. Rev. D, 94, 103006
Neronov, A., Savchenko, D., & Semikoz, D. V. 2024, Phys. Rev. Lett., 132, 101002
Petropoulou, M., Sironi, L., Spitkovsky, A., & Giannios, D. 2019, ApJ, 880, 37
Readhead, A. C. S. 1994, ApJ, 426, 51
Shepherd, M. C. 1997, in Astronomical Society of the Pacific Conference Series, 125, Astronomical Data Analysis Software and Systems VI, eds. G. Hunt, & H. Payne, 77
Sikora, M., Begelman, M. C., & Rees, M. J. 1994, ApJ, 421, 153
Sironi, L., Giannios, D., & Petropoulou, M. 2016, MNRAS, 462, 48
Spada, M., Ghisellini, G., Lazzati, D., & Celotti, A. 2001, MNRAS, 325, 1559
Stecker, F. W., Done, C., Salamon, M. H., & Sommers, P. 1991, Phys. Rev. Lett., 66, 2697
Zhang, X., Xiong, D.-r., Gao, Q.-g., et al. 2024, MNRAS, 529, 3699